CMLS, Cell. Mol. Life Sci. 60 (2003) 1224–1234
1420-682X/03/061224-11
DOI 10.1007/s00018-003-3057-0

CMLS Cellular and Molecular Life Sciences

Research Article

Mapping the antigenicity of copper-treated cellular prion protein with the scrapie isoform

B.-S. Wong[a], R. Li[a], J. Sassoon[b], S.-C. Kang[a], T. Liu[a], T. Pan[a], N. S. Greenspan[a], T. Wisniewski[c], D. R. Brown[b] and M.-S. Sy[a,*]

[a] Institute of Pathology (BRB 933), Case Western Reserve University, School of Medicine, 10900 Euclid Ave., Cleveland, Ohio 44106 (USA), Fax +1 216 3681357. e-mail: mxs92@po.cwru.edu
[b] Department of Biology and Biochemistry, Bath University, Bath (United Kingdom)
[c] Department of Neurology and Pathology, New York University, School of Medicine, New York (USA)

Received 13 February 2003; received after revision 21 March 2003; accepted 24 March 2003

Abstract. When recombinant and cellular prion protein (PrP^C) binds copper, it acquires properties resembling the scrapie isoform (PrP^{Sc}), namely protease resistance, detergent insolubility and increased β sheet content. However, whether the conformations of PrP^C induced by copper and PrP^{Sc} are similar has not been studied in great detail. Here, we use a panel of seven monoclonal antibodies to decipher the epitopes on full-length mouse PrP^C that are affected by exogenous copper, and to compare the antigenicity of the copper-treated full-length PrP^C with the full-length PrP^{Sc} present in scrapie-infected mouse brains. In the presence of copper, we found that epitopes along residues 115–130 and 153–165 become more accessible on PrP^C. These regions correspond to the two β sheet strands in recombinant PrP and they were proposed to be important for prion conversion. However, when we compared the antibody-binding patterns between full-length PrP^C with full-length PrP^{Sc} and between copper-treated full-length PrP^C with full-length PrP^{Sc}, antibody binding to residues 143–155 and 175–185 was consistently increased on PrP^{Sc}. Collectively, our results suggest that copper-treated full-length PrP^C does not resemble full-length PrP^{Sc}, despite acquiring PrP^{Sc}-like properties. In addition, since each full-length protein reacts distinctively to some of the antibodies, this binding pattern could discriminate between PrP^C and PrP^{Sc}.

Key words. Prion protein; copper; epitope mapping; antigenicity.

The conformational conversion of the α-helical cellular prion protein (PrP^C) to a β sheet protease resistant scrapie isoform termed PrP^{Sc} is believed to be the key event in the pathogenesis of prion diseases, including Creutzfeldt-Jakob disease (CJD) in humans and scrapie in animals [1]. Along the N terminus of mammalian prion protein lies a highly conserved octarepeat motif [2]. This sequence binds copper atoms [3–5] with affinities estimated to be between micromolar [6] and fentomolar [7].

The tertiary structure of the protease-sensitive recombinant mouse [8], Syrian hamster [9], bovine [10] and human [11] PrP have been determined by nuclear magnetic resonance spectroscopy. All these recombinant proteins showed the C-terminal domain along residues 124–231 folded into a core comprising three α helices, up to two short β strands and an intradisulfide bridge connecting the second and third helices. Conversely, the N-terminal portion of the protein (residues 23–124) appears highly flexible and devoid of any regular secondary structure under the experimental conditions where no copper was bound to the octarepeats. However, when copper binds to recombinant PrP, it could instigate conformational changes along this sequence [7, 12].

Under certain conditions, binding of copper to recombinant PrP causes a dramatic increase in β sheet content and the protein becomes protease resistant [12, 13]. Similarly,

* Corresponding author.

PrP^C from an in vitro cell model, transgenic mice and human brain microsomes also becomes protease resistant and detergent insoluble when exogenous copper is added [13, 14]. These three features, namely increased β sheet content, protease resistance and detergent insolubility, are major properties of PrP^{Sc} [1]. Furthermore, exogenous copper has been reported to facilitate the acquisition of infectivity and protease resistance by inactivated PrP^{Sc} in vivo [15]. All these lines of evidence suggest that copper could be crucial in the conversion process. However, a recent study showed that while copper-treated transgenic mouse PrP^C with an engineered 3F4 epitope binds well to antibody 3F4, PrP species from scrapie-infected hamster brains do not [14]. Based on these observations, the authors concluded that copper-treated transgenic mouse PrP^C, while possessing certain PrP^{Sc}-like properties, has a different conformation from hamster PrP^{Sc}.

Although little is known about PrP^{Sc} conformation, antibody mapping of PrP^C and the resistant core of PrP^{Sc} termed PrP27–30 suggested structural differences along residues 90–120 [16]. Moreover, antibody binding to residues 133–157, comprising helix A in PrP^C, could inhibit prion propagation in vitro [17, 18] and in vivo [19]. In vitro studies using synthetic peptides have also identified residues 119–136, 166–179 and 200–223 on PrP^C to be important in the conversion process [20].

In this paper, we used a panel of seven anti-PrP monoclonal antibodies (mAbs) [21, 22] to probe potential global and local conformational changes induced by exogenous copper on brain-derived full-length mouse PrP^C. In addition, we extend our analysis to compare the antibody-binding pattern of full-length native mouse PrP^C with or without copper treatment to the full-length PrP^{Sc} from infected mouse brains.

Materials and methods

Mice

Four brains each from FVB mice, prion knockout (*Prnp*$^{-/-}$) mice [23] and CD1 mice infected with the scrapie strain ME7 [24] were used in individual analyses. All experiments were performed in triplicate. Preparations of 20% (w/v) brain homogenates and the measurement of total brain proteins were as previously reported [25].

Recombinant mouse prion protein

Cloning, expression and purification of recombinant mouse prion protein spanning residues 23–231 (recmoPrP23–231) have been described [4, 12]. The nucleotides encompassing the C-terminal hexahistidine purification tag within the plasmid constructs [12] were removed by PCR-based site-directed mutagenesis [26] using the splint primer pair; 5′-cgggagaagatcctgagagca ccacc-3′ and 5′-ggtggtgctctcaggatcttctcccg-3′. Purified proteins were filtered through a 30,000 MWCO concentrator (Amicon) to remove high-molecular-weight im purities, before they were concentrated with a 10,000 MWCO concentrator (Amicon). Protein concentration was determined by spectrophotometry. The purified rec-moPrP23–231 was folded to an α helical structure [12] and analysis showed it to be free of copper atoms [4].

Antibodies

The epitopes of the seven anti-PrP mAbs used in this study are depicted in figure 1. The methods used for the production and characterization of these mAbs have been described [21, 27]. mAb 8B4 recognizes an epitope along the unstructured N terminus region at residues 34–45, 11G5 reacts with residues 115–130 covering β sheet 1, 7H6 recognizes residues 130–140, 7A12 interacts with helix A between residues 143–155, 2C2 reacts with residues 153–165 covering β sheet 2, and 8H4 recognizes residues 175–185 of helix B. mAb 9H7 only reacts with an epitope on a long peptide encompassing residues 143–231. mAbs 8B4, 7A12, 2C2, 8H4 and 9H7 are of IgG1 subtype, whereas mAbs 11G5 and 7H6 are IgG2b subtype. Biotinylation of mAbs was performed using the EZ-linked Sulfo-NHS-Biotin kit (Pierce Endogen) according to the manufacturer‘s recommendation.

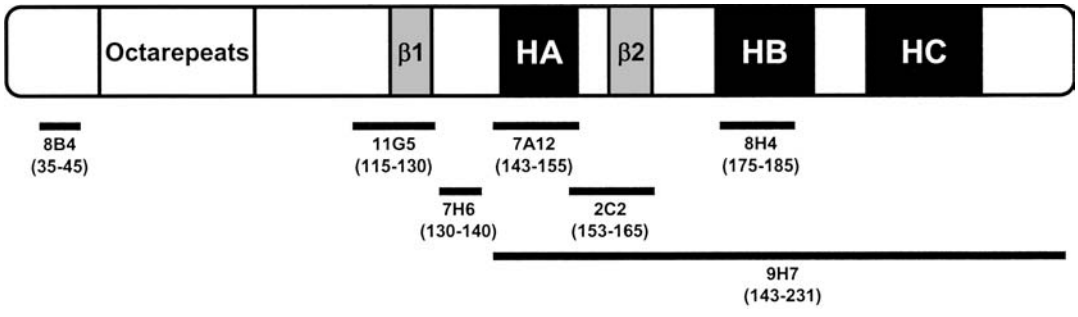

Figure 1. Antibody epitope location on mouse prion protein. Schematic representation of the three α helices (HA, HB, HC) and two β strands (1, 2), represented by black and gray boxes, respectively, on the linear sequence of recombinant mouse prion protein from residues 23–231. Location of the known epitopes for antibodies 8B4, 11G5, 7H6, 2C2, 7A12, 8H4 and 9H7 are given in parentheses.

Immunoprecipitation, protease digestion and immunoblotting

Brain-derived prion proteins were immunoprecipitated by mixing total brain homogenate with mAb 8B4 at 4 °C overnight [28]. Rec-moPrP23–231 was immunoprecipitated by incubating the recombinant PrP with mAb 8B4 using the above conditions. Protein-antibody complexes were bound to protein G-agarose beads (Roche Diagnostic) by rocking at 4 °C for 3 h. The beads were washed three times with phosphate-buffered saline (PBS) and the supernatant aspirated after spinning at 10,000 rpm for 2 min at 4 °C. The beads were finally suspended in SDS gel sample buffer (Novex) and boiled for 10 min at 95 °C for electrophoresis.

To determine protease-resistant, PrP species in total brain homogenates or immunoprecipitations were incubated with 100 µg/ml proteinase K (Roche Diagnostic) at 37 °C for 1 h before stopping the reaction with 1 mM phenylmethylsulfonyl fluoride (PMSF) (Roche Diagnostic) [29]. Proteins were precipitated with 4 vol of ice-cold methanol at –20 °C for 1 h followed by centrifugation at 13,000 g for 10 min at 4 °C. The supernatant was carefully removed and the pellet resuspended with SDS gel-loading buffer (Novex) before being denatured for 10 min at 95 °C for separation.

Immunoblotting was performed according to an earlier report [25]. The membrane was probed with mAbs 8B4 and 8H4 [22], exposed to horseradish peroxidase (HRP)-conjugated anti-mouse Fc (Chemicon) and visualized using the POD chemiluminescence kit (Roche Diagnostic). Prestained protein standards (Bio-Rad) were used to determine the apparent molecular weights of the protein bands.

Protein deglycosylation

The enzymatic procedure was performed as described elsewhere [28] with recombinant peptide N-glycosidase F (PNGase F, New England Biolabs). Treated proteins were precipitated with 4 vol of ice-cold methanol at –20 °C for 1 h. After spinning at 13,000 g for 10 min at 4 °C, the supernatant was carefully removed and the pellet resuspended with SDS gel-loading buffer before being denatured for 10 min at 95 °C for electrophoresis.

Quantifying brain-derived full-length PrP

Different dilutions of total brain homogenates from individual brains (n = 4 each) of normal and ME7-infected mice were analyzed alongside known quantities of rec-moPrP23–231 [30] with SDS-PAGE followed by immunoblotting using mAb 8B4 [22], which reacts with full-length PrP [28]. The content of full-length PrP in individual mouse brain homogenates was calculated from the slope of the linear curve, based on known amounts of rec-moPrP23–231, obtained from the absorbance-concentration relationship determined by densitometry (Scion Image for Windows, beta 4.0.2).

Titrating antibody binding to recombinant mouse prion protein

Microtiter plates (Corning) were coated with 200 ng of mAb 8B4 in PBS before washing using PBS with 0.1% Tween 20 (PBST). Unbound sites were blocked with 4% non-fat milk in PBST for 1 h at room temperature with gentle agitation, and subsequently rinsed with PBST. One hundred nanograms of purified rec-moPrP23–231 folded into an α helical conformation [12] was added in quadruplicate to respective wells and the plate incubated overnight at 4 °C. After three washes using PBST, various concentrations of biotinylated mAbs 11G5, 7H6, 2C2, 8H4, 7A12 and 9H7 were added to designated wells and incubated for 2 h at room temperature with gentle agitation. The plate was washed before incubating with HRP-conjugated streptavidin (BD Pharmingen) diluted 1 : 1000 in PBST at room temperature. After washing, 1 mg/ml of 2,2′-azino-di-[3-ethylbenzthiazoline sulfonate] (ABTS) solution (Roche Diagnostic) was added to the wells before measuring the absorbance at 405 nm. The antibody concentration for individual mAbs that gave 50% binding to available sites on rec-moPrP23–231 was calculated [30].

Sandwich ELISA for full-length PrP

Microtiter plates (Corning) were coated overnight at 4 °C with 200 ng of mAb 8B4 in PBS before washing with PBST [30]. Unbound sites were blocked using 4% non-fat milk in PBST before washing. Individual brain homogenates containing ~100 ng of full-length native PrP^{C} or PrP^{Sc} were added in triplicate to respective wells and incubated overnight at 4 °C. After washing, PBS (pH 7.4) or 50, 150 or 300 µM of $CuSO_4$ in PBS, pH 7.4, was added to designate wells for overnight incubation at room temperature with gentle agitation. At least three washes with PBST were performed before adding biotinylated mAbs to designated wells. The concentrations of individual biotinylated mAbs that gave 50% maximum occupancy of the available sites on rec-moPrP23–231 were used (11G5, 49 ng/ml; 7H6, 50 ng/ml; 2C2, 627 ng/ml; 8H4, 52 ng/ml; 9H7, 50 ng/ml; 7A12, 64 ng/ml). The plate was washed, incubated with HRP-conjugated streptavidin (BD Pharmingen) for 1 h followed by another round of washing before adding ABTS solution as described above. Absorbance was read at 405 nm. mAb 8B4-coated wells not in contact with brain homogenates but incubated either with PBS or the examined $CuSO_4$ concentrations served as controls. Absorbance readings obtained from these controls were subtracted from the readings of the appropriate PrP-containing wells.

Statistical analysis

Significant differences for the conformational immunoassay were analyzed using paired-sample two-tailed

Student's t-test. A p value of ≤ 0.05 was considered significant.

Results

Prion protein expression

Prior to carrying out the antibody-mapping studies we established the patterns of prion protein expression in normal and infected brains, as well as the binding specificity of our anti-PrP mAbs. In one-dimensional immunoblots, PrP^C from normal brains separates into three major bands thought to represent the diglycosylated, monoglycosylated and unglycosylated isoforms [31]. Recent studies, however, suggested that in human brains, these bands correspond to full-length and various N-terminally truncated PrP^C species [28]. We therefore used two anti-PrP mAbs to delineate mouse PrP^C expression before and after PNGase F cleavage [28] (fig. 2A). Without PNGase F treatment, mAb 8H4, which binds along residues 175–185, reacts with three major bands (35, 32 and 28 kDa) (lane 3) whereas mAb 8B4 recognizing sequence between residues 34–45 reacts predominantly with the 35-kDa band (lane 1). After deglycosylation, mAb 8B4 also detected a single band but at a lower molecular weight of 28 kDa (lane 2), which corresponds to deglycosylated, full-length PrP^C. In contrast, mAb 8H4 reacts with two major bands of 28 and 18 kDa (lane 4). These results are consistent with our earlier studies in non-prion-afflicted human brains [28], which indicate that some of these PrP^C species are N-terminally truncated. Moreover, our results also clearly demonstrated that mAb 8B4 only reacts with the full-length PrP^C species, while mAb 8H4 reacts with full-length and N-terminus-truncated PrP^C species.

On the other hand, in the homogenates prepared from ME7-infected brains, mAb 8H4 detected at least four major bands ranging from 20 to 35 kDa (fig. 2B, lane 4). Proteinase K (PK) digestion resolved the PrP population to three major bands of 28, 24 and 20 kDa (lane 5) whereas PNGase treatment resulted in two apparent bands of 28 and 20 kDa, and a very faint band around 26–27 kDa (lane 6).

In normal mouse brains, mAb 8B4 reacted with one predominant 35-kDa protein (fig. 2A, lane 1). However, mAb 8B4 constantly recognized two major bands of 35 and 32 kDa together with a very faint species at ~30 kDa in the infected brains (fig. 2B, lane 1). No immunoreactivity was detected after PK proteolysis (lane 2) in line with studies indicating that the N terminus of all PrP species is sensitive to protease digestion [1, 32]. After deglycosylation, only a single population of 28-kDa protein was detected (lane 3). Our results therefore suggested that differences in N-linked glycans were the cause of the dissimilarity in the molecular weights of the full-length PrP species seen in infected brain. These observations are

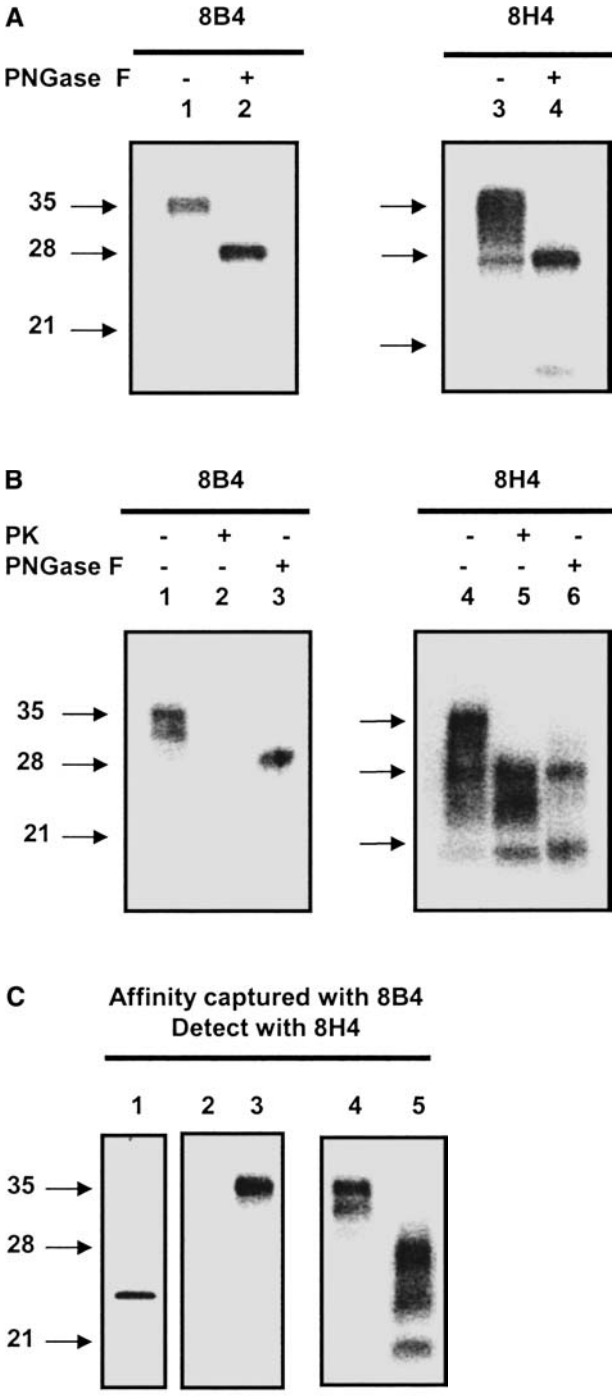

Figure 2. Mouse prion protein expression. (*A*) PrP species in 100 µg of normal mouse brain homogenate without (lanes 1, 3) or with (lanes 2, 4) PNGase F treatment were immunodetected using mAbs 8B4 (lanes 1, 2) and 8H4 (lanes 3, 4). (*B*) Mouse PrP species in 50 µg of ME7-infected brain homogenate (lanes 1, 4), digested with proteinase K (lanes 2, 5) or treated with PNGase F (lanes 3, 6), before immunoblotting with mAbs 8B4 (lanes 1–3) and 8H4 (lanes 4–6). (*C*) Rec-moPrP23–231 (lane 1), brain homogenates from prion protein knockout ($Prnp^{-/-}$) (lane 2) and wild-type (lane 3) mice were immunoprecipitated with mAb 8B4 before detecting using mAb 8H4. Full-length PrP species immunoprecipitated with mAb 8B4 from ME7-infected brains without (lane 4) or with (lane 5) proteinase K digestion before they were immunoblotted using mAb 8H4. The apparent molecular weight is given in kDa.

in total agreement with our findings in human CJD, where we observed more full-length PrP species with distinct N-linked glycans [33].

To firmly establish that mAb 8B4 reacts solely with the full-length PrP species, we next immunoprecipitated PrP species from normal and infected brains, and recombinant mouse PrP (rec-moPrP23–231) with the N terminus mAb 8B4 and then immunoblotted the captured PrP species with the C terminus mAb 8H4 (fig. 2C). In normal brains, only one distinct band was detected (lane 3) instead of the three PrP bands observed (fig. 2A, lane 3) without immunoprecipitation. These results clearly indicate that only full-length PrP^{C} was immunoprecipitated. The specificity of this procedure was confirmed by the lack of PrP immunoreactivity in the brain homogenate from prion protein knockout (*Prnp*$^{-/-}$) mice (fig. 2C, lane 2) mixed with mAb 8B4 and immunoblotted using mAb 8H4. On the other hand, rec-moPrP23–231 similarly treated was observed as a single 24-kDa band (lane 1).

As with whole-brain homogenates detected with mAb 8B4 (fig. 2B, lane 1), three PrP bands were detected with the C terminus mAb 8H4 after confinity capturing the PrP species from infected brains with mAb 8B4 (lane 4). These again confirm that there were at least three full-length PrP species differing in their N-linked glycans (fig. 2B, lanes 1, 3). When we subjected these full-length PrP species immunoprecipitated from infected brains to PK treatment, three major bands of 28, 24 and 20 kDa were detected (fig. 2C, lane 5). Consistent results were also obtained when these PK-treated samples were immunoblotted with biotinylated anti-PrP mAb 7A12 (data not shown). These results attest that the affinity-captured, full-length PrP species from infected brains were the protease-resistant scrapie isoform (PrP^{Sc}).

Antibody binding to recombinant mouse prion protein

We next carried out a series of titration experiments to identify the saturating concentration for each of the six detecting biotinylated mAbs using rec-moPrP23–231 [12]. The purified rec-moPrP23–231 used in this experiment was folded in an α-helical structure [12] and has no detectable copper atoms [4]. Microtiter plates were first coated with mAb 8B4 before adding 100 ng of rec-moPrP23–231 onto the wells. Different amounts of biotinylated anti-PrP mAb (11G5, 7H6, 2C2, 8H4, 9H7 or 7A12) were then added to detect the bound rec-moPrP23–231. Except for mAb 2C2, all the biotinylated anti-PrP mAbs reached binding saturation with less than 300 ng/ml of antibody (fig. 3). On the other hand, biotinylated mAb 2C2 binding along residues 153–165 attained saturation only at a concentration of ~2500 ng/ml (fig. 3). This could be due either to weaker immunoreactivity by mAb 2C2, or the epitope in question is less accessible on rec-moPrP23–231. Titrating mAbs binding to the rec-moPrP23–231 indicated that 50% occupancy of available sites on the recombinant protein was achieved at concentrations of 49 ng/ml for 11G5, 50 ng/ml for 7H6, 627 ng/ml for 2C2, 52 ng/ml for 8H4, 50 ng/ml for 9H7 and 64 ng/ml for 7A12. These concentrations were used in all subsequent experiments.

Antibody reactivity to recombinant and full-length native PrP^{C}

To determine if our panel of anti-PrP mAbs bind comparably to rec-moPrP23–231 and brain-derived full-length PrP^{C}, we incubated a similar quantity of each protein onto ELISA wells pre-coated with mAb 8B4. Bound PrP was detected using titrated concentrations of biotinylated mAbs 11G5, 7H6, 2C2, 7A12, 8H4 and 9H7 (fig. 3). A broadly similar antibody-binding pattern was observed between our rec-moPrP23–231 and native PrP^{C} from normal mouse brains (data not shown). Although the mAb 8H4 epitope encompassed one of the two N-linked glycosylation sites, the antibody bound equally well with rec-moPrP23–231 and full-length PrP^{C}. This observation suggests that mAb 8H4 reactivity is independent of the post-translational modification. In agreement with our results, studies using a different panel of anti-PrP Fab also reported similar binding between recombinant PrP and transfected cell surface PrP^{C} [34].

Antibody mapping of copper-induced changes on native PrP^{C}

We next used the capture-ELISA to investigate whether addition of exogenous copper to full-length native PrP^{C} results in changes in the binding of the mAbs. However, when copper reacts with hydrogen peroxide, it has been reported to generate reactive oxygen species that can cleave PrP at the N terminal [35]. We therefore first determined whether incubation of full-length PrP species from normal or infected brains in the presence of 50, 150 or 300 µM copper will result in cleavage at the N terminus. We did not detect any truncation of the N terminus (data not shown) when the proteins were immunoblotted with the N-terminus-specific mAb 8B4.

In addition, we and others have previously established that in contrast to weakly acidic conditions [12], at neutral pH, equivalent amounts of copper can also bind to recombinant and native PrP^{C} after refolding [5, 36, 37]. After capturing full-length native PrP^{C} with plate-bound mAb 8B4, unbound PrP species were removed before different concentrations (50, 150 and 300 µM) of $CuSO_4$ in PBS (pH 7.4) were then added to the ELISA wells. Repeated washing with PBST has not been shown to affect the bound Cu on rec-moPrP23–231 [4] and native PrP^{C} [36]. The binding of various epitopes on the bound PrP^{C} was then determined with different biotinylated anti-PrP mAbs. The concentrations of biotinylated mAbs used were derived from titration experiments (fig. 3) that gave

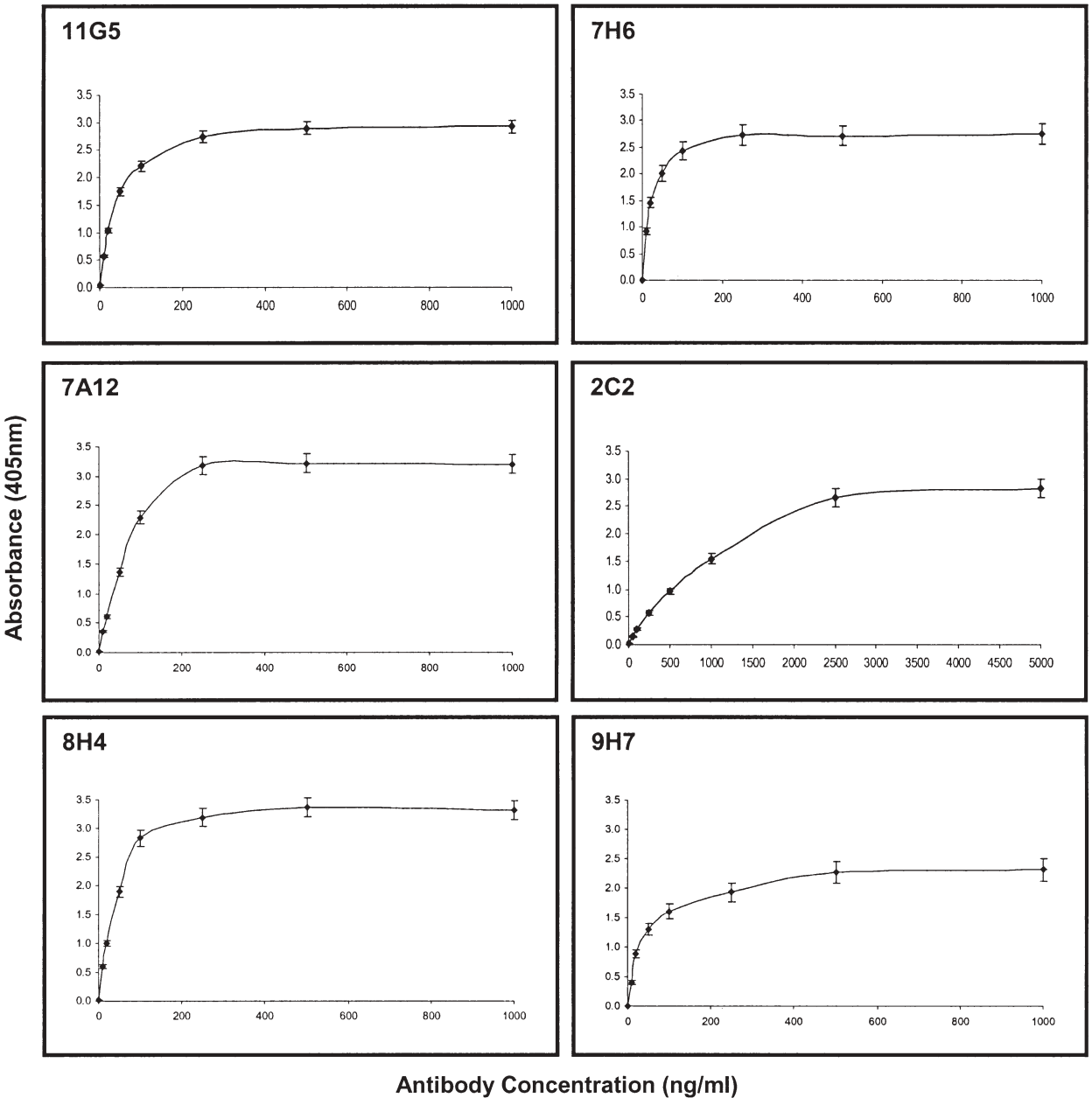

Figure 3. Titrating antibody reactivity on recombinant mouse prion protein. Antibody titration using 100 ng of rec-moPrP23–231 captured with 200 ng of coated mAb 8B4 against various concentrations of biotinylated mAbs 11G5, 7H6, 2C2, 8H4, 7A12 and 9H7. The antibody concentrations for individual biotinylated anti-PrP mAbs that give 50% binding to available sites on rec-moPrP23–231 folded into an α helical conformation were determined and used to analyze relative binding in subsequent conformation-sensitive immunoassays.

50% maximum binding to available sites on rec-moPrP23–231.

When full-length native PrP^C was incubated with copper, significant changes in the binding of mAbs 11G5, 2C2 and 7A12 were detected (fig. 4). While reactivities of mAbs 2C2 and 11G5 were significantly elevated by up to 70 and 163%, respectively, in a copper-concentration-dependent manner, the binding of mAb 7A12 was only marginally increased. mAb 11G5 binds along residues 115–130 covering the first β strand and mAb 2C2 recognizes the second β strand between residues 153–165 (fig. 1). Copper had no effect on mAb 7H6, 8H4 and 9H7 binding to the captured protein. These results suggest that the effect of copper is regionally specific and does not drastically alter the overall conformation of PrP^C.

Comparative antibody binding to full-length PrP^C, copper-treated full-length PrP^C and full-length PrP^{Sc}

We next determined the binding of the mAbs to full-length PrP^C and copper-treated full-length PrP^C from un-

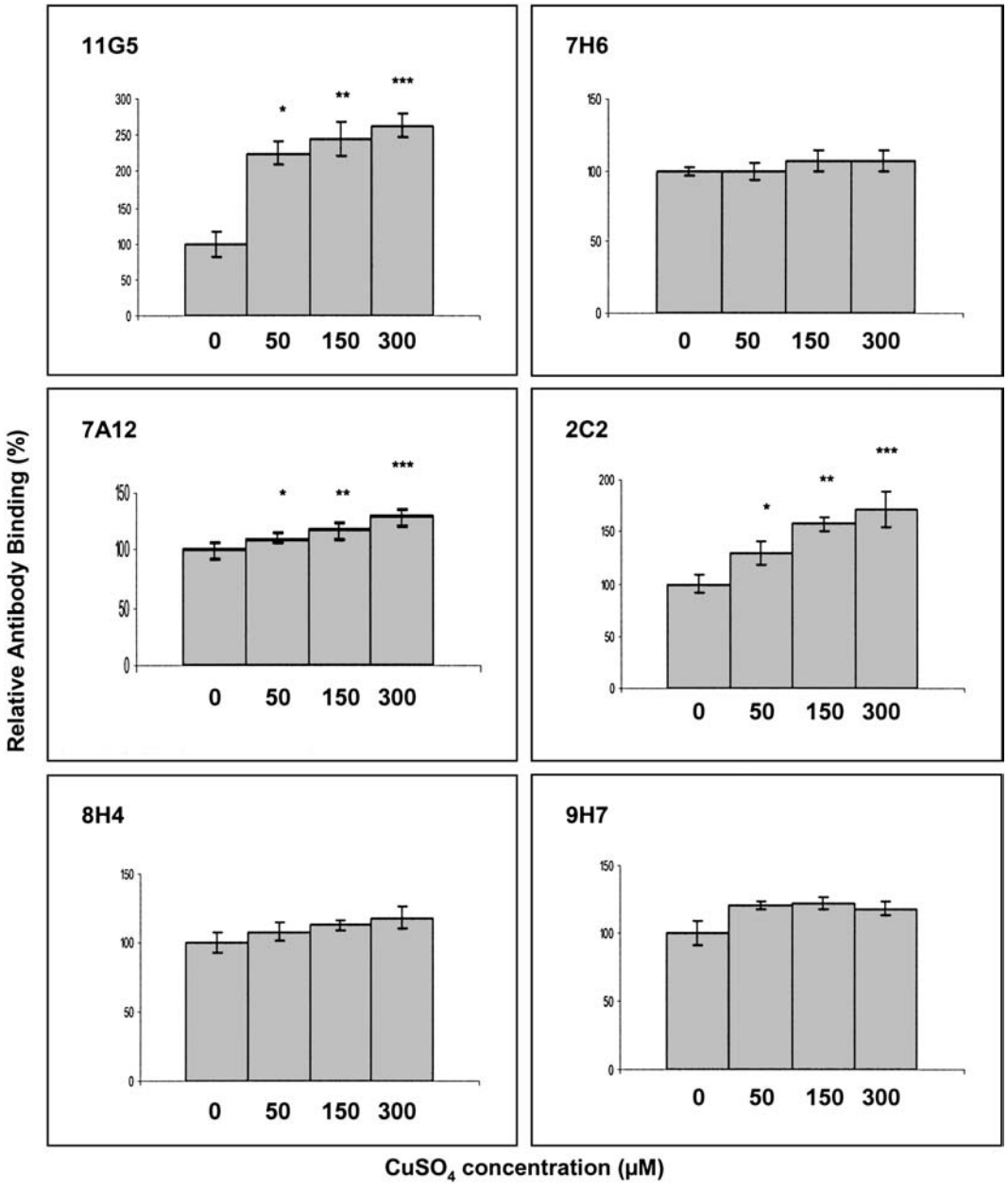

Figure 4. Copper-induced changes in antibody reactivity to full-length PrP^{C}. Full-length PrP^{C} from normal mouse brains was captured with coated mAb 8B4. Bound PrP^{C} was incubated with PBS (pH 7.4) or 50, 150, 300 µM $CuSO_4$ in PBS (pH 7.4) before detection with biotinylated anti-PrP mAbs as described in Materials and methods. Antibody binding is given as a percentage of the binding signal correlated with the untreated (PBS) sample that was arbitrarily set at 100%. The data presented are the mean ± SE of four mouse brains each performed in triplicate. Significant differences in antibody reactivity between untreated (PBS) and 50 µM (*), 150 µM (**) or 300 µM (***) $CuSO_4$-treated samples (Student's t test, $p \leq 0.05$).

infected brains with the full-length PrP^{Sc} from ME7-infected brains. We incubated each brain homogenate containing ~100 ng of full-length PrP as determined by densitometry onto ELISA wells pre-coated with mAb 8B4. The captured PrPC from normal brains was then incubated overnight with PBS or with 50, 150 or 300 µM $CuSO_4$ in PBS as described earlier. Full-length PrP^{Sc} was incubated in PBS identically. After extensive washing, the availability of various epitopes on the bound PrP was determined with different biotinylated anti-PrP mAbs as before. Since the binding patterns of the six biotinylated mAbs to full-length PrP^{C} treated with 50, 150 or 300 µM $CuSO_4$ are similar (data not shown), only the binding profile of the protein incubated with 50 µM $CuSO_4$ is presented in our comparisons.

To simplify our comparison, we divided the mAbs into two groups based on the proximity of their epitopes to determine the binding ratio of these mAbs on individual

proteins, namely full-length PrP^C, copper-treated full-length PrP^C and full-length PrP^{Sc}. Group 1 consists of mAbs 11G5 and 7H6 and group 2 comprises mAbs 7A12, 2C2 and 8H4. We defined the binding ratio of group 1 mAbs as the ratio of OD405 for (7H6/11G5) while for group 2 mAbs, the OD405 ratio was for (8H4/2C2) and (7A12/2C2).

Group 1 mAbs bond to full-length PrP^C with a binding ratio of 3.2 and for group 2 mAbs, a binding ratio of 1.4 and 1.1 for (8H4/2C2) and (7A12/2C2), respectively, was found (fig. 5A). When PrPC was treated with 50 µM copper, the group 1 binding ratio was dramatically reduced to 1.2 (fig. 5B), reflecting a pronounced increase in mAb 11G5 binding (fig. 4). In contrast, addition of 50 µM copper only marginally reduced the binding ratios for group 2 mAbs (8H4/2C2 = 0.9, 7A12/2C2 = 0.7) due to an increase in mAb 2C2 reactivity (fig. 4). Full-length PrP^{Sc} on the other hand had a binding ratio of 1.9 for group 1 mAbs (fig. 5C), a ratio intermediate between full-length PrP^C and copper-treated full-length PrP^C. However, binding ratios of group 2 mAbs to full-length PrP^{Sc} were greatly increased (8H4/2C2 = 3.3, 7A12/2C2=2.6) contributed by greater binding with mAbs 8H4 and 7A12. Taken together, these results indicate that full-length PrPC, copper-treated full-length PrPC and full-length PrPSc have different antigenicities (table 1).

Discussion

In this study, we used a panel of seven anti-PrP antibodies [21, 27, 28] to gain insights into the conformational changes induced by copper on full-length PrP^C from normal mouse brains. We also extended our analysis to compare these conformations with the full-length mouse PrP^{Sc} from brains infected with the well-characterized scrapie strain ME7 [24]. These studies were made possible because we have gathered a panel of anti-PrP mAbs that react with epitopes extending from the N to the C terminus of PrP^C. Unlike an earlier report which examined total PrP species [14], we focused our studies on full-length PrP species because most if not all the copper binding occurs at the N terminus of the molecule [5, 7]. To achieve this, we used mAb 8B4 to capture only the full-length native PrP^C and PrP^{Sc} in normal and infected brains, respectively.

While mAb 8B4 recognizes a single PrP population in normal brains, it reacts with three full-length PrP species with different N-linked glycans in scrapie-infected brains. Although enzymatic deglycosylation will resolve the full-length PrP^{Sc} to a single population, the procedure required the proteins to be denatured [28]. Since denaturation will inactivate and alter PrP^{Sc} conformation [15], we have to forgo this process. Nevertheless, this observation is similar to our recent studies of human sporadic CJD [33] where we consistently detect more full-length PrP species in infected brains than in normal control brains. The reasons why infected brains have more full-length PrP species are not known. One possible explanation for this finding is that these species are preferentially synthesized during prion infection [38]. Alternatively, the degradation of these species may be impaired in infected brains.

An important question that needs to be addressed is whether our studies truly reflect the in vivo binding of copper to the full-length PrP species. While our purified recombinant PrP does not contain any detectable traces of copper atoms [4], in vitro studies have shown that the recombinant protein can bind up to five copper atoms per molecule [3, 5, 7]. Although native PrP^C has been reported to contain about three copper atoms per molecule [36], we do not know whether this stoichiometry is uniform in all PrP^C species (full-length and N-terminal-truncated PrP^C) or whether it can vary between PrP species, for example some PrP^C having three or more copper atoms, while other PrPs have none. Furthermore, native PrP^C can still bind immobilized copper resin [39, 40], indicating that not all copper-binding sites are occupied on the protein. Taken together, these results provide strong evidence that both recombinant PrP and native PrP^C have unoccupied metal-binding sites that can be saturated with exogenous copper.

Table 1. Binding ratio of anti-PrP mAbs on brain-derived full-length PrP^C, copper-treated full-length PrP^C and full-length PrP^{Sc}.

	Group 1		Group 2		
mAbs	11G5	7H6	7A12	2C2	8H4
Epitope	115–130	130–140	143–155	153–165	175–185
Binding ratio	7H6/11G5		7A1/2C2	8H4/2C2	
PrP^C	3.2		1.1	1.4	
Cu-treated PrP^C	1.2		0.7	0.9	
PrP^{Sc}	1.9		2.6	3.3	

The MAbs were divided into two groups based on the proximity of their epitopes (given in fig. 1) to determine the binding ratio of these mAbs on individual proteins.

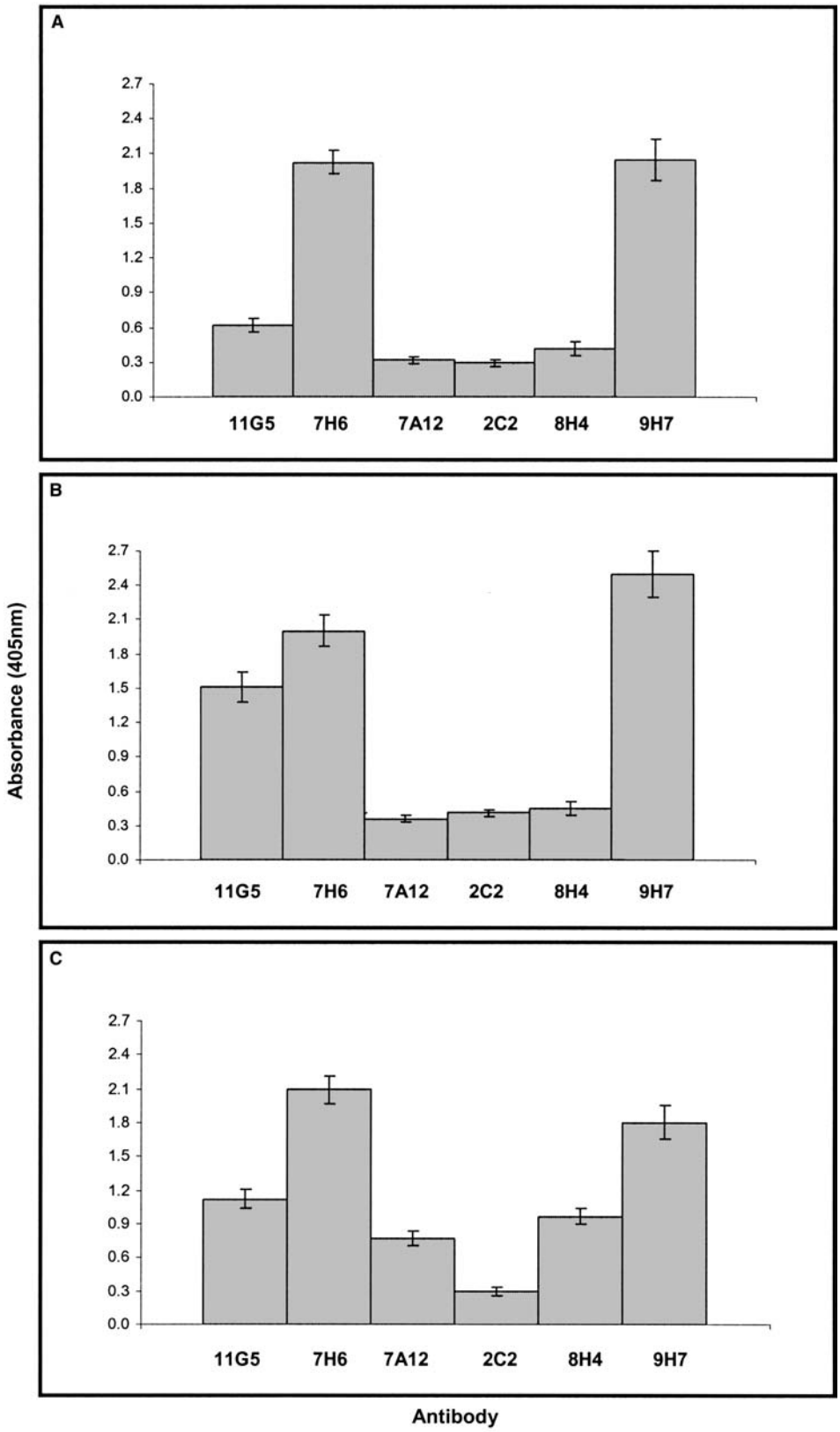

Figure 5. Antibody binding to full-length native mouse PrP^{C} and PrP^{Sc}. One hundred nanograms of full-length PrP^{C} from normal (*A*, *B*) and PrP^{Sc} from ME7-infected mouse brains (*C*), as determined by densitometry, was affinity captured with 200 ng of coated mAb 8B4. Bound PrP^{C} from (*B*) was incubated with 50 µM $CuSO_4$ in PBS (pH 7.4) or with PBS alone to (*A*, *C*) before they were detected using biotinylated anti-PrP mAbs as described in Materials and methods. The data presented are the mean ± SEM of four mouse brains each performed in triplicate.

In the current study, we found that two epitopes located along residues 115–130 and 153–165 on full-length native PrP^C become more accessible following interaction with copper as shown by increased binding of mAbs 11G5 and 2C2. The epitope recognized by mAb 11G5 covered the first β strand whereas mAb 2C2 recognized the second β strand, based on the structural information derived from recombinant mouse PrP [8]. Of interest is that residues 111–138 are highly conserved among mammalian *Prnp* genes that have been sequenced [41]. This high degree of conservation suggests that the region may be important in the physiologic functions of PrP^C. Importantly, both regions affected by copper do in part overlap with the some of the sequences thought to be crucial in prion conversion [16–18, 20].

When we compared the antibody-binding pattern between full-length PrP^C with full-length PrP^{Sc} and between copper-treated full-length PrP^C with the full-length PrP^{Sc}, mAbs 7A12 and 8H4 appeared to bind differently. The epitopes of mAbs 7A12 and 8H4 were apparently better presented on the full-length PrP^{Sc} from infected brain. Indeed, antibody binding to the sequence encompassing the mAb 7A12 epitope can inhibit prion propagation [17–19]. Also worth noting is that mAb7A12 shows increased reactivity with the PrP^{Sc} species in bovine-spongiform-encephalopathy-infected brains [G. Barnard and M.-S. Sy, unpublished data]. On the other hand, copper has no effect on the binding of mAbs 7A12 and 8H4 on full-length PrP^C. Although the reasons why copper-treated full-length PrP^C has a different conformation from full-length PrP^{Sc} in infected brain are not known, the presence of two additional full-length PrP^{Sc} species in infected brain may in part contribute to this disparity. Alternatively, the difference in the affinity toward copper between the PrP species in normal and infected brains [40, 42, 43] may also contribute to the conformational differences suggested by our mAbs.

In summary, we identified two regions, corresponding to the two β sheet strands in rec-moPrP23–231 [8], on full-length native PrP^C that are most susceptible to the effects of exogenous copper. Intriguingly, although these regions overlapped with those suggested to modulate the pathogenic conversion of PrP^C to PrP^{Sc}, we observed that copper-treated full-length PrP^C binds differently to a panel of six anti-PrP antibodies when compared to the full-length PrP^{Sc} in infected brains. These differences in antibody-binding suggest that the conformation induced by copper on full-length PrP^C can be distinguished from full-length PrP^{Sc}. In addition, our comparisons of the antibody binding pattern of full-length PrP^C with or without copper treatment and full-length PrP^{Sc} indicate that copper-treated full-length PrP^C may represent an intermediate conformer between full-length PrP^C and full-length matured PrP^{Sc}. Finally, since each protein produces different antibody-binding patterns, these distinctions may serve as an 'antibody profile' for discriminating between full-length PrP^C and PrP^{Sc}.

Acknowledgements. D. R. B. thanks Dr. J. Manson (Institute for Animal Health, Edinburgh, UK) for providing the prion protein knockout (*Prnp*$^{-/-}$) mice. B.-S. W. thanks Dr. K. Qin (Toronto University, Canada) for enlightening discussion. This work was supported in part by a contract from the Prions Development Labs Inc. (M.-S. S.), grants from the National Institutes of Health and the Alzheimer's Association (T. W.), and a Grant-in-Aid of Research from Sigma Xi, The Scientific Research Society (B.-S. W.). D. R. B. was supported by a Fellowship from the UK Biotechnology and Biological Science Research Council. B. S. W. was supported by a Fellowship from the Singapore National Medical Research Council.

1 Prusiner S. B. (1998) Prions. Proc. Natl. Acad. Sci. USA **95:** 13363–13383
2 Wopfner F., Weidenhufer G., Schneider R., Brunn A. von, Gilch S., Schwarz T. F. et al. (1999) Analysis of 27 mammalian and 9 avian PrPs reveals high conservation of flexible regions of the prion protein. J. Mol. Biol. **289:** 1163–1178
3 Brown D. R., Qin K., Herms J. W., Madlung A., Manson J., Strome R. et al. (1997) The cellular prion protein binds copper in vivo. Nature **390:** 684–687
4 Brown D. R., Wong B. S., Hafiz F., Clive C., Haswell S. and Jones I. M. (1999) Normal prion protein has an activity like that of superoxide dismutase. Biochem. J. **344:** 1–5
5 Qin K., Yang Y., Mastrangelo P. and Westaway D. (2002) Mapping Cu(II) binding sites in prion proteins by diethyl pyrocarbonate modification and matrix-assisted laser desorption ionization-time of flight (MALDI-TOF) mass spectrometric footprinting. J. Biol. Chem. **277:** 1981–1990
6 Stockel J., Safar J., Wallace A. C., Cohen F. E. and Prusiner S. B. (1998) Prion protein selectively binds copper(II) ions. Biochemistry **37:** 7185–7193
7 Jackson G. S., Murray I., Hosszu L. L., Gibbs N., Waltho J. P., Clarke A. R. et al. (2001) Location and properties of metal-binding sites on the human prion protein. Proc. Natl. Acad. Sci. USA **98:** 8531–8535
8 Riek R., Hornemann S., Wider G., Glockshuber R. and Wuthrich K. (1997) NMR characterization of the full-length recombinant murine prion protein, mPrP(23-231). FEBS Lett. **413:** 282–288
9 Donne D. G., Viles J. H., Groth D., Mehlhorn I., James T. L., Cohen F. E. et al. (1997) Structure of the recombinant full-length hamster prion protein PrP(29–231): the N terminus is highly flexible. Proc. Natl. Acad. Sci. USA **94:** 13452–13457
10 Lopez Garcia F., Zahn R., Riek R. and Wuthrich K. (2000) NMR structure of the bovine prion protein. Proc Natl Acad Sci USA **97:** 8334–8339
11 Zahn R., Liu A., Luhrs T., Riek R., Schroetter C. von, Lopez Garcia F. et al. (2000) NMR solution structure of the human prion protein. Proc. Natl. Acad. Sci. USA **97:** 145–150
12 Wong B. S., Venien-Bryan C., Williamson R. A., Burton D. R., Gambetti P., Sy M. S. et al. (2000) Copper refolding of prion protein. Biochem. Biophys. Res. Commun. **276:** 1217–1224
13 Qin K., Yang D. S., Yang Y., Chishti M. A., Meng L. J., Kretzschmar H. A. et al. (2000) Copper(II)-induced conformational changes and protease resistance in recombinant and cellular PrP: Effect of protein age and deamidation. J. Biol. Chem. **275:** 19121– 19131
14 Quaglio E., Chiesa R. and Harris D. A. (2001) Copper converts the cellular prion protein into a protease resistant species that is distinct from the scrapie isoform. J. Biol. Chem. **276:** 11432–11438

15 McKenzie D., Bartz J., Mirwald J., Olander D., Marsh R. and Aiken J. (1998) Reversibility of scrapie inactivation is enhanced by copper. J. Biol. Chem. **273:** 25545–25547
16 Peretz D., Williamson R. A., Matsunaga Y., Serban H., Pinilla C., Bastidas R. B. et al. (1997) A conformational transition at the N terminus of the prion protein features in formation of the scrapie isoform. J. Mol. Biol. **273:** 614–622
17 Enari M., Flechsig E. and Weissmann C. (2001) Scrapie prion protein accumulation by scrapie-infected neuroblastoma cells abrogated by exposure to a prion protein antibody. Proc. Natl. Acad. Sci. USA **98:** 9295–9299
18 Peretz D., Williamson R. A., Kaneko K., Vergara J., Leclerc E., Schmitt-Ulms G. et al. (2001) Antibodies inhibit prion propagation and clear cell cultures of prion infectivity. Nature **412:** 739–743
19 Heppner F. L., Musahl C., Arrighi I., Klein M. A., Rulicke T., Oesch B. et al. (2001) Prevention of scrapie pathogenesis by transgenic expression of anti-prion protein antibodies. Science **294:** 178– 182
20 Horiuchi M., Baron G. S., Xiong L. W. and Caughey B. (2001) Inhibition of interactions and interconversions of prion protein isoforms by peptide fragments from the C-terminal folded domain. J. Biol. Chem. **276:** 15489–15497
21 Li R., Liu T., Wong B. S., Pan T., Morillas M., Swietnicki W. et al. (2000) Identification of an epitope in the C terminus of normal prion protein whose expression is modulated by binding events in the N terminus. J. Mol. Biol. **301:** 567–573
22 Liu T., Zwingman T., Li R., Pan T., Wong B. S., Petersen R. B. et al. (2001) Differential expression of cellular prion protein in mouse brain as detected with multiple anti-PrP monoclonal antibodies. Brain Res. **896:** 118–129
23 Manson J. C., Clarke A. R., Hooper M. L., Aitchison L., McConnell I. and Hope J. (1994) 129/Ola mice carrying a null mutation in PrP that abolishes mRNA production are developmentally normal. Mol. Neurobiol. **8:** 121–127
24 Carp R. I., Meeker H., Sersen E. and Kozlowski P. (1998) Analysis of the incubation periods, induction of obesity and histopathological changes in senescence-prone and senescence-resistant mice infected with various scrapie strains. J. Gen. Virol. **79:** 2863–2869
25 Wong B. S., Liu T., Li R. L., Pan T., Petersen R. B., Smith M. A. et al. (2001) Increased levels of oxidative stress markers detected in the brains of prion knock-out mice. J. Neurochem. **76:** 565–572
26 Brown D. R., Iordanova I. K., Wong B. S., Venien-Bryan C., Hafiz F., Glasssmith L. L. et al. (2000) Functional and structural differences between the prion protein from two alleles prnpa and prnpb of mouse. Eur. J. Biochem. **267:** 2452–2459
27 Zanusso G., Liu D., Ferrari S., Hegyi I., Yin X., Aguzzi A. et al. (1998) Prion protein expression in different species: analysis with a panel of new mAbs. Proc. Natl. Acad. Sci. USA **95:** 8812–8816
28 Pan T., Li, R., Wong B. S., Liu T., Gambetti P., and Sy M. S. (2002) Heterogeneity of normal prion protein in two-dimensional immunoblot: presence of various glycosylated and truncated forms. J. Neurochem. **81:** 1092–1101
29 Wong B. S., Brown D. R., Pan T., Whiteman M., Liu T., Bu X. et al. (2001) Oxidative impairment in scrapie-infected mice is associated with brain metals perturbations and altered antioxidant activities. J. Neurochem. **79:** 689–698
30 Harlow E. and Lane D. (1999) Using Antibodies: A Laboratory manual, Cold Spring Harbor Laboratory Press, Cold Spring Harbor, N. Y.
31 Caughey B., Race R. E., Ernst D., Buchmeier M. J., and Chesebro B. (1989) Prion protein biosynthesis in scrapie-infected and uninfected neuroblastoma cells. J. Virol. **63:** 175–181
32 Parchi P., Zou W., Wang W., Brown P., Capellari S., Ghetti B. et al. (2000) Genetic influence on the structural variations of the abnormal prion protein. Proc. Natl. Acad. Sci. USA **97:** 10168–10172
33 Pan T., Colucci M., Wong B. S., Li R., Liu T., Petersen R. B. et al. (2001) Novel differences between two human prion strains revealed by two-dimensional gel electrophoresis. J. Biol. Chem. **276:** 37284–37288
34 Williamson R. A., Peretz D., Pinilla C., Ball H., Bastidas R. B., Rozenshteyn R. et al. (1998) Mapping the prion protein using recombinant antibodies. J. Virol. **72:** 9413–9418
35 McMahon H. E. M., Mange A., Nishida N., Creminon C., Casanova D. and Lehmann S. (2001) Cleavage of the amino terminus of the prion protein by reactive oxygen species. J. Biol. Chem. **276:** 2286–2291
36 Brown D. R., Clive C. and Haswell S. J. (2001) Anti-oxidant activity related to copper binding of native prion protein. J. Neurochem. **76:** 69–76
37 Daniels M. and Brown D. R. (2002) Purification and preparation of prion protein: synaptic superoxide dismutase. Methods Enzymol. **349:** 258–267
38 Russelakis-Carneiro M., Saborio G. P., Anderes L. and Soto C. (2002) Changes in the glycosylation pattern of prion protein in murine scrapie: Implications for the mechanism of neurodegeneration in prion diseases. J. Biol. Chem. **277:** 36872–36877
39 Pan K. M., Stahl N. and Prusiner S. B. (1992) Purification and properties of the cellular prion protein from Syrian hamster brain. Protein Sci. **1:** 1343–1352
40 Shaked Y., Rosenmann H., Hijazi N., Halimi M. and Gabizon R. (2001) Copper binding to the prp isoforms: a putative marker of their conformation and function. J. Virol. **75:** 7872–7874
41 Schatzl H. M., Da Costa M., Taylor L., Cohen F. E. and Prusiner S. B. (1995) Prion protein gene variation among primates. J. Mol. Biol. **245:** 362–374
42 Wadsworth J. D. F., Hill A. F., Joiner S., Jackson G. S., Clarke A. R. and Collinge J. (1999) Strain-specific prion-protein conformation determined by metal ions. Nat Cell Biol **1:** 55–59
43 Wong B. S., Chen,S. G., Colucci M., Xie Z., Li R., Pan T. et al. (2001) Aberrant metal binding by prion protein in human prion disease. J. Neurochem. **78:** 1400–1408